

FIRST winged radio galaxies with X and Z symmetry

SOUMEN BERA,¹ SABYASACHI PAL,^{2,3} TAPAN K. SASMAL,¹ AND SOUMEN MONDAL¹

¹*Department of Physics, Jadavpur University, Kolkata, 700032, India*

²*Midnapore City College, Kuturiya, Bhadutala, Paschim Medinipur, West Bengal, 721129, India*

³*Indian Centre for Space Physics, 43 Chalantika, Garia Station Road, 700084, India*

Submitted to ApJSupplSer

ABSTRACT

X-shaped radio galaxies are a subclass of radio sources that exhibit a pair of secondary low surface brightness radio lobes oriented at an angle to the primary high surface brightness lobes. Sometimes, the secondary low brightened lobes emerge from the edges of the primary high brightened lobes and form a Z-symmetric morphology. We present a systematical search result for X-shaped radio galaxies (XRGs) and Z-shaped radio galaxies (ZRGs) from the VLA Faint Images of the Radio Sky at Twenty-Centimeters (VLA FIRST) Survey at 1.4 GHz. Our search yields a total of 296 number of radio sources, out of which 161 are XRGs and 135 are ZRGs. We have also made optical identification of these sources from the different available literature. J1124+4325 and J1319+0502 are the farthest known XRG and ZRG, respectively. We have estimated spectral index and radio luminosity of these radio sources and made a comparative study with previously detected XRGs and ZRGs. The average value of luminosities for XRGs is higher than that of ZRGs. With the help of a large sample size of the newly discovered XRGs and ZRGs, various statistical properties of these sources are studied. Out of 161 XRGs presented in the current paper, 70% (113) are FR II radio galaxies and 13% (20) are FR I radio galaxies. For 28 XRGs, the morphology is complex and could not be classified. For XRGs, the statistical studies are done on the angle between the major axis and minor axis and the relative size of the major and minor axes. For the ZRGs a statistical study is done on the angular size.

Keywords: Active galactic nuclei (16); Catalogs (205); Jets (870); Quasars (1319); Radio continuum emission (1340); Surveys (1671)

1. INTRODUCTION

A typical double-lobed radio galaxy morphology shows a pair of radio jets, each one directed in the opposite direction from the central black hole (BH) or active galactic nuclei (AGN). The alignment of the primary jets gives a linear structure in radio map. A small number of subclasses are found with a nonlinear special structure. ‘Winged’ radio galaxies is a subclass where two additional secondary lobes (wings) are found beside the primary lobes. These symmetric and low luminosity extrusion of plasma extend at an angle from the center to a distance nearly equal to or lower than the length of the active lobes. Based on the alignment of the secondary lobes with the primary lobes, two subclasses are defined, ‘X’-shaped radio galaxies (XRGs) and ‘Z/S’-shaped radio galaxies (ZRGs). For XRGs, both the sets of lobes pass symmetrically through the center of the elliptical galaxy that

is the source of the lobes. In the case of ZRGs, the secondary lobes are seen from the edges of the primary jets.

The first reported radio galaxy with wings is 3C 272.1 (Riley 1972), which showed a Z-like structure. Later NGC 326 also showed Z-like structure with possible precessing beams (Ekers et al. 1978). The elliptical galaxy NGC 3309 (Dreyer 1888) was identified as the X-shaped source by Kotanyi (1990). Leahy & Parma (1992) first classified sources with X-shapes as XRGs and presented a list of 11 objects with wings. Cheung (2007) (C07 afterwards) first made a systematic study to look for radio galaxies with wings and identified 100 XRG candidates using the VLA Faint Images of the Radio Sky at Twenty-centimeters (FIRST) survey. Later, (Yang et al. (2019) Y19 afterwards) also identified 290 winged radio galaxies from the FIRST survey. Bhukta et al. (2020) discovered 50 XRGs and tens of ZRGs from the TIFR GMRT Sky Survey (TGSS) at 150 MHz. By using an automated morphological classification scheme to the FIRST radio sources, Proctor (2011) identified 156 XRG candidates out of which 21 sources had already been reported in C07.

The maximum number of these sources are of Fanaroff-Riley type II (FR II; (Fanaroff & Riley 1974)) and the remaining are either FR I or mixed (Merritt & Ekers 2002).

The origin of the wings in XRGs is still an arguable topic. There are several models available to explain the mechanism behind the formation of this exotic type of sources (Rottmann 2001; Dennett-Thorpe et al. 2002). The proposed models are: (a) the backflow of plasma (Leahy & Williams 1984; Capetti et al. 2002), the secondary wings result from backflow of plasma from the hot spots of the active lobes into the surrounding asymmetric medium; (b) a merger of two black holes (Rottmann 2001; Merritt & Ekers 2002): The coalescence of two super-massive black holes (SMBHs) is another possibility for the origin of the X-shaped radio morphology; (c) realignment of a central SMBH-accretion disk system (Dennett-Thorpe et al. 2002), the secondary lobes in XRGs may be the remnants left over from a rapid realignment of a central SMBH-accretion disk system; and (d) precession of twin jets (Mack et al. 1994). It is important to note that none of the above-mentioned models can explain the properties of all the XRGs.

The studies made by C07 and Y19 are far from complete within the FIRST coverage area because both of the studies concentrated on a selected subset of the survey depending on the high dynamic range. C07 also looked for only those sources that are larger than $15''$. Naturally many of the X-shaped sources within the FIRST survey area are missed due to above-mentioned restrictions. We made a complete study to search for all possible XRGs and ZRGs within the FIRST survey area.

In section 2, we have described source identification method. In section 3, we described different properties of XRGs (section 3.3) and ZRGs (section 3.4). General discussion on different results are made in section 4 and in section 5, concluding remarks are made.

We have used the following cosmology parameters for the entire discussion in this paper: $H_0 = 67.4 \text{ km s}^{-1} \text{ Mpc}^{-1}$, $\Omega_m = 0.315$ and $\Omega_{vac} = 0.685$ (Aghanim et al. 2018). These cosmological constants are estimated using final full-mission Planck measurements of the cosmic microwave background (CMB) anisotropies, combining information from the temperature and polarization maps and the lensing reconstruction.

2. IDENTIFICATION OF THE XRGs AND ZRGs

2.1. The FIRST Survey Data

The FIRST survey (White et al. 1996) covers a radio sky of 10,575 square degrees of the north and south Galactic caps near 1400 MHz (21 cm). This survey has a typical RMS of 0.15 mJy and an angular resolution of $5''$ (Becker et al. 1995). The FIRST survey area covers approximately 25% of the total sky, out of which, approximately 80% is in the north Galactic cap (8444 square degrees), and remaining 20% is in the south Galactic cap (2131 square degrees) (Becker et al. 1995). The FIRST survey offers better resolution and sensitivity than the previous NRAO Very Large Array (VLA) Sky Survey (NVSS) at 1.4 GHz, which uses VLA D con-

figuration and covers 82% of the celestial sphere with angular resolution $45''$ and an RMS of $\sim 0.45 \text{ mJy}$ (Condon et al. 1998). The FIRST survey uses the NRAO VLA in its B configuration (VLA B). The FIRST sky is mapped with three minute snapshots covering a hexagonal grid using $2 \times 7 \times 3$ MHz frequency channels centered at 1365 and 1435 MHz until 2011¹. After 2011, the updated Expanded Very Large Array (EVLA) receiver came, which results in few changes in survey procedures. Frequencies of 1335 and 1730 MHz were used after 2011 with a one minute iteration using $2 \times 64 \times 2$ MHz frequency channels. The cleaning and calibration of the raw data are done using an automated pipeline based largely on routines in the Astronomical Image Processing System (AIPS)². The latest version of FIRST data (2017 December 14) is used. This version covers R.A. = 07.0h to 17.5h, decl. = -08.0 deg to $+57.6 \text{ deg}$ in northern sky and R.A. = 20.4hr to 4.0hr, decl. = -11.5 deg to $+15.4 \text{ deg}$ in southern sky.

With the relatively high sensitivity and resolution of the FIRST survey, it is possible to study the morphology of faint radio galaxies in detail. The earlier FIRST database was used to search for radio galaxies with different distinct morphologies such as head tailed sources (Missaglia et al. 2019; Sasmal et al. 2020), hybrid morphology radio sources (Gopal-Krishna & Wiita 2000), compact steep spectrum sources and core-dominated triple sources (CSS; Kunert et al. (2002); Marecki et al. (2006)), giant radio sources (GRSs; Kuźmicz et al. (2018)), and double-double radio galaxies (DDRG; Proctor (2011)). Earlier, about 390 winged radio galaxy candidates were discovered using part of FIRST database Cheung (2007); Yang et al. (2019). Here we are reporting a complete search of the FIRST database to look for radio galaxies with X and Z symmetries.

2.2. Search Strategy

We looked for X-shaped and Z-shaped radio sources using the VLA FIRST survey database. The catalog contains a total of 946,432 radio sources. We filtered all sources in the catalog that have an angular size of $>10''$ (i.e. at least twice the convolution beam size). Our filtering gives an output of 95,243 sources. We visually inspected fields of all the sources ($>10''$) to look for new candidate radio galaxies with wings. From the limited-resolution FIRST images ($\sim 5''$), we confidently classified a sufficient number of objects as having the characteristic wing lengths of $>80\%$ of the active lobes. Following C07, we have also included galaxies with shorter wings ($< 80\%$ wing-to-lobe length ratios), as it is probable that projection effects are important. Since secondary jets are often diffused and weak and often lack bright peaks at the end (hotspots), it is difficult to measure the extent of these jets.

Earlier, C07 restricted search for X-shaped radio galaxies for fields with high dynamic ranges and $> 15''$ source

¹ <http://sundog.stsci.edu/first/description.html>

² <http://info.cv.nrao.edu/aips/>

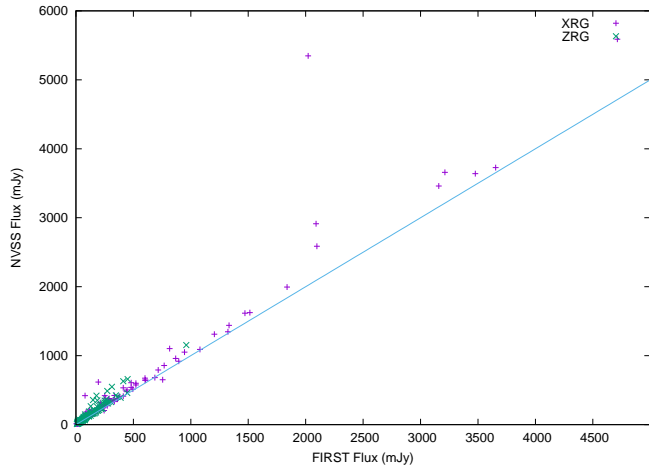


Figure 1. Flux densities measured from the FIRST catalog and the NVSS catalog are shown for all XRGs and ZRGs presented in this paper.

sizes. Y19 also restricted the search depending on the dynamic range. For the restricted search criterion, both of the studies missed many of the candidate *X*-shaped galaxies. C07 and Y19 manually searched 1648 and 5128 probable sources, in contrast to the probable 95,243 sources searched by the present paper.

2.2.1. Definition of XRGs and ZRGs

The wings in radio galaxies appear as the secondary lobes. Depending on the position of the wings, we classified the winged radio sources in two groups: XRGs and ZRGs. For the “*X*”-shaped radio sources, the wings (secondary lobes) appeared to be coming from the central spot or from near the central region. Here we define the near central region as the region covered by $\sim 25\%$ of the primary jet length from the central spot. The sources are tagged as the *Z/S*-shaped radio source when the secondary lobes appear to come from the edges of the primary jet or the non-near central region. The morphology of sources depend on how many radio contours we consider and hence on the signal to noise. To make a uniform study, we started contours from 0.25 mJy for all images.

2.2.2. The Optical Counterparts and Properties

We have searched for the optical/IR counterpart for each of the newly discovered XRGs and ZRGs from the Sloan Digital Sky Survey (SDSS) data catalog (Gunn et al. 2006), the Digital Sky Survey (DSS), and the NASA/IPAC Extragalactic Database³. The optical/IR counterpart identification was based on the optical/IR source position relative to the

radio galaxy morphology. We overlaid images from the FIRST survey with DSS2 red images. We have used the position of the optical/IR counterpart of XRGs and ZRGs as the position of these sources. Optical/IR counterparts are found for 98 sources out of a total of 161 sources for the case of *X*-shaped galaxies and 88 sources out of 135 sources for the case of *Z*-shaped sources, respectively. For objects with no clear optical/IR counterparts, we have used the location of the core of the radio galaxy or the intersection of both radio lobes as the position of these sources. We found that out of 135 redshift values, 123 are spectroscopic (91%) and the rest 12 are photometric. Within 72 redshift measurements of XRGs, 67 are spectroscopic and 5 are photometric. Out of 63 redshift measurements of ZRGs, 56 are spectroscopic and 7 are photometric. Except otherwise stated, all redshifts are taken using SDSS catalog, release 12.

3. RESULT

We report the discovery of 161 new XRGs and 135 new ZRGs. This discovery helps to significantly increase the number of this kind of sources. The larger samples of XRGs and ZRGs help us to do study various statistical properties of these sources, the result of which is described in the following subsections.

All candidates of the XRGs and ZRGs are cataloged in Table ?? and ??, respectively. For completeness, we have also included 21 XRG candidates and 44 ZRG candidates in these tables from Proctor (2011), which we independently identified following our method. In Figure 1, the flux-density measurement of all XRGs and ZRGs are shown using FIRST and NVSS catalogs. For most of the sources, the flux density measured from the NVSS image is significantly higher than the corresponding measurement from the FIRST image. While the mean and median flux-density measurements from the NVSS catalog are 448.5 and 155 mJy, the mean and median flux densities from the measurements of the FIRST catalog are 381 and 122 mJy. Due to high resolution and lack of antennas in short spacing, the FIRST survey is prone to flux-density loss. For flux-density measurement of the sources reported in the present paper in 1400 MHz, we have used corresponding images from NVSS. The lower-resolution VLA configuration D was used for the NVSS (with a resolution of $\sim 45''$), compared to B configuration of the FIRST survey (with a resolution of $\sim 5''$), which means NVSS is better suited in detecting the most extended radio structure. NVSS counterparts are found for each of the sources, though due to less resolution, the *X*-shape and *Z*-shape are not evident from any of the NVSS images of these sources. For five XRGs (J0742+3339, J0932+1610, J1104+2828, J2218+0012 and J2324+1438) and two ZRGs (J0847+3147 and J1138+2039), we measure the 1400 MHz flux density from FIRST instead of NVSS as for these sources there were other background sources in the FIRST image inside the beam size of the NVSS image.

In column 5 of Table 1 and Table 2, we have mentioned the catalog name from where the optical counterpart is found. The redshifts (z) of these sources are also mentioned when

³ <https://ned.ipac.caltech.edu>

available (in column 6). We have also calculated the corresponding flux density of each source at 150 MHz (column 8) using TGSS [Intema et al. \(2017\)](#). We have calculated two-point spectral index between 150 and 1400 MHz (α_{150}^{1400}) when flux density at 150 MHz is available and tabulated them in 9th column of Table 1 and 2. In columns 10 and 11, the linear size and luminosity of the sources are tabulated for the sources with known redshifts. In the last column, we have mentioned the name of other catalogs in radio wavelengths where these sources were mentioned earlier without detection of them as XRGs or ZRGs.

In Figure 2, we have shown the example of 12 XRGs, and in Figure 3, we have shown the example of 12 ZRGs. The DSS2 red optical images are overlayed with the FIRST radio images. Synthesized beams are shown in one corner of the images.

3.1. Spectral Index (α)

We have calculated the two-point spectral index of newly discovered sources between 150 and 1400 MHz (assuming $S_\nu \propto \nu^\alpha$, where S_ν is the radiative flux density at a given frequency, ν , and α is the spectral index) and mentioned them in Table 1 and Table 2. Spectral index measurements are available for 107 XRGs and 79 ZRGs. For the rest of the sources, due to higher RMS in the images of TGSS, the sources were not detectable in 150 MHz map of TGSS.

Figure 4 shows histogram with the spectral index distribution of sources presented in the current article for XRGs (left) and ZRGs (right). The plot shows that the total span of α_{150}^{1400} is from -0.35 to -1.05 for XRGs and -0.14 to -1.21 for ZRGs. Among XRGs, J2249+0209 has the lowest spectral index with $\alpha_{150}^{1400} = -1.05$ and J0758+4406 has the highest spectral index with $\alpha_{150}^{1400} = -0.35$. Among ZRGs, J1325+5736 have the lowest spectral index with $\alpha_{150}^{1400} = -1.21$ and J1524+1627 has the highest spectral index with $\alpha_{150}^{1400} = -0.14$. Most of the radio galaxies show steep radio spectrum $\alpha \leq -0.5$, as expected from the lobe dominated radio source. There is a clear distinction between peaks in the histogram for XRGs and ZRGs. For XRGs, the histogram shows two peaks near -0.55 and -0.7 , and for ZRGs, the histogram shows a peak near -0.65 .

3.2. Radio Luminosity (L_{rad})

The radio luminosities (L_{rad}) of newly discovered XRGs and ZRGs are calculated using

$$L_{rad} = 1.2 \times 10^{27} D_{\text{Mpc}}^2 S_0 \nu_0^{-\alpha} (1+z)^{-(1+\alpha)} \times (\nu_u^{(1+\alpha)} - \nu_l^{(1+\alpha)}) (1+\alpha)^{-1} \text{erg s}^{-1} \quad (1)$$

where D_{Mpc} is luminosity distance to the source (Mpc), S_0 is the flux density (Jy) at a given frequency, ν_0 (Hz); z is the redshift of the radio galaxy; and α is the spectral index ($S \propto \nu^\alpha$). ν_u (Hz) and ν_l (Hz) are the upper and lower cutoff frequencies ([O'Dea & Owen 1987](#)). In our calculation, we

assume the upper and lower cutoff frequencies as 100 GHz and 10 MHz, respectively.

In Figure 5, we plot the distribution of radio luminosities of XRGs and ZRGs presented in the current paper with known redshifts (z). We have performed a Kolmogorov-Smirnov test ([Peacock 1983](#); [Smirnov 1948](#)) between the distribution of XRGs and ZRGs and found they are consistent with each other with $D = 0.52$ and $p\text{-value} = 8 \times 10^{-7}$. The radio luminosity of the sources at 1.4 GHz is in the order of 10^{43} erg s^{-1} , which is bit less than a typical radio galaxy. The average value of Luminosity in [Nilsson et al. \(1993\)](#), which is a collection of 540 double radio sources, is $\text{Log } L$ [erg s^{-1}] is 44.07. The average value of $\text{Log } L$ is higher for XRGs compared to ZRGs. For XRGs, the average value of $\text{Log } L$ [erg s^{-1}] is 43.24 (1σ standard deviation=1.05, median=43.31) and that of ZRGs is 42.42 (1σ standard deviation=0.58, median=42.42).

The most luminous XRG in our sample is J1124+4325 with $L_{rad} = 7.76 \times 10^{44}$ erg s^{-1} and the most luminous ZRG in our sample is J1156+2138 with $L_{rad} = 4.70 \times 10^{43}$ erg s^{-1} . The least luminous XRG in our sample is J1354+5840 with $L_{rad} = 3.19 \times 10^{38}$ erg s^{-1} and the least luminous ZRG in our sample is J1140+1743 with $L_{rad} = 7.2 \times 10^{40}$ erg s^{-1} .

3.3. Properties of XRGs

Most of the XRGs are found to be FR II radio galaxies ([Leahy & Parma 1992](#); [Cheung 2007](#); [Yang et al. 2019](#)). This trend is strengthened by the present catalog of XRGs. Out of 161 XRGs presented in the current paper, 70% (113) are FR II radio galaxies and 13% (20) are FR I radio galaxies. For 28 XRGs, the jet morphology is complex and could not be classified. For the uniform classification of sources, we used radio maps starting from 0.25 mJy contour. Depending on the position of peak flux in lobes of the major axis, we classified the source as FR I and FR II. Figure 6 shows a histogram indicating the number of XRGs with FR I and FR II type. For none of the XRGs in the present sample, the secondary lobes are FR II type.

3.3.1. Major and Minor Axes

In Figure 7, the angular size of the major axis of X-shaped radio galaxies for the angular size of the corresponding minor axis is plotted. The angular sizes depend on the lowest contour of the image. For uniformity, we have started contours from 0.25 mJy for images of all XRGs. For 27 galaxies in our list, the minor axis is elongated in only one direction. These 27 galaxies are not included in Figure 7.

In Figure 8, we have shown a histogram with the distribution of ratio between the minor and major axes of radio galaxies with "X-like shape", as presented in this paper. Out of 161 radio galaxies included in the Figure, 47 radio galaxies has secondary jets with 50 – 75% of the size of the primary jets. For 32 radio galaxies, the secondary jets are with 75 – 100% size of the primary jet. For seven XRGs, the secondary jets are bigger than the primary jets. Here we should remember that primary jets also could be affected by the effect of projection.

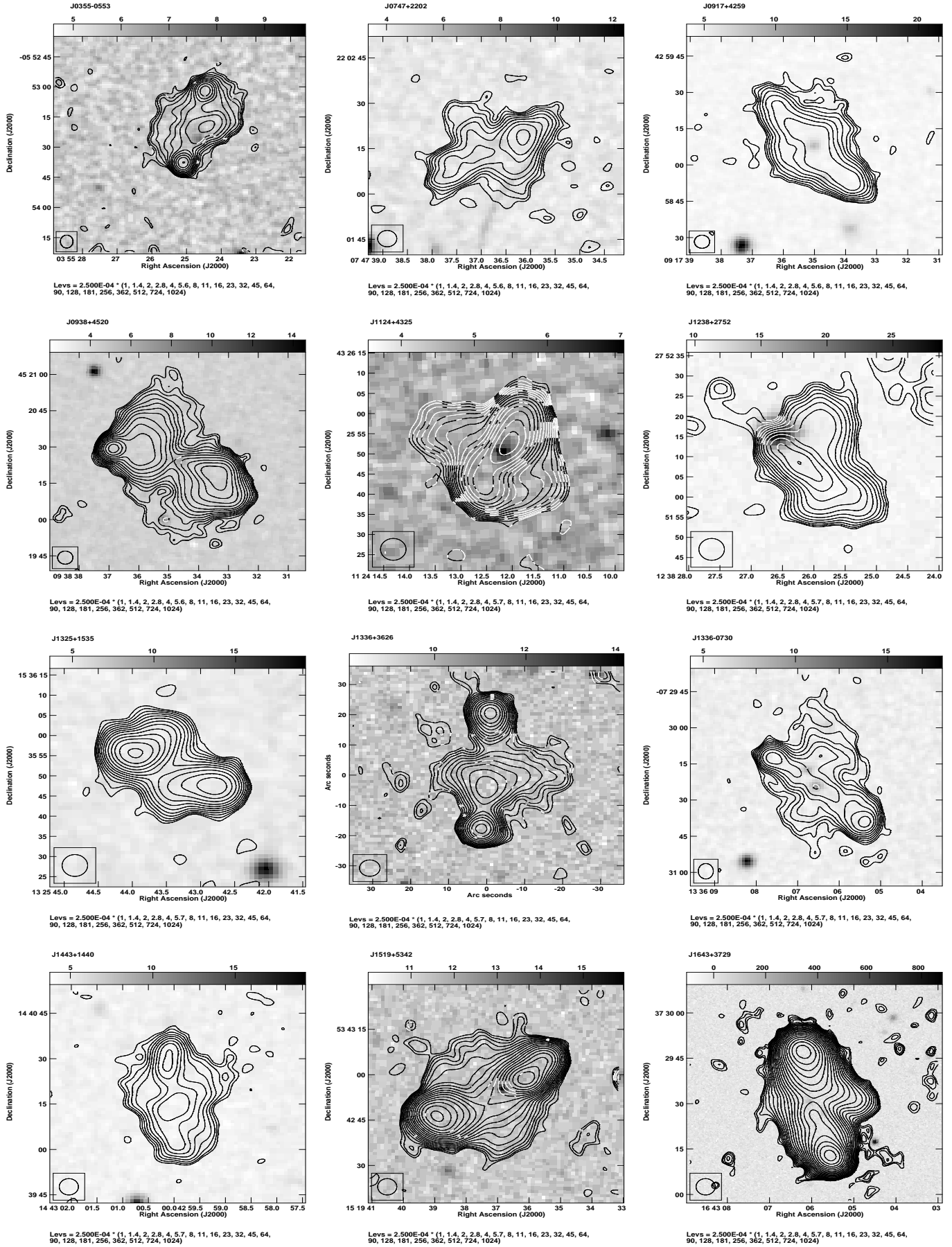


Figure 2. The FIRST image of a sample of 12 "X"-shaped radio sources (contours) overlaid on the DSS2 red image (grey scale).

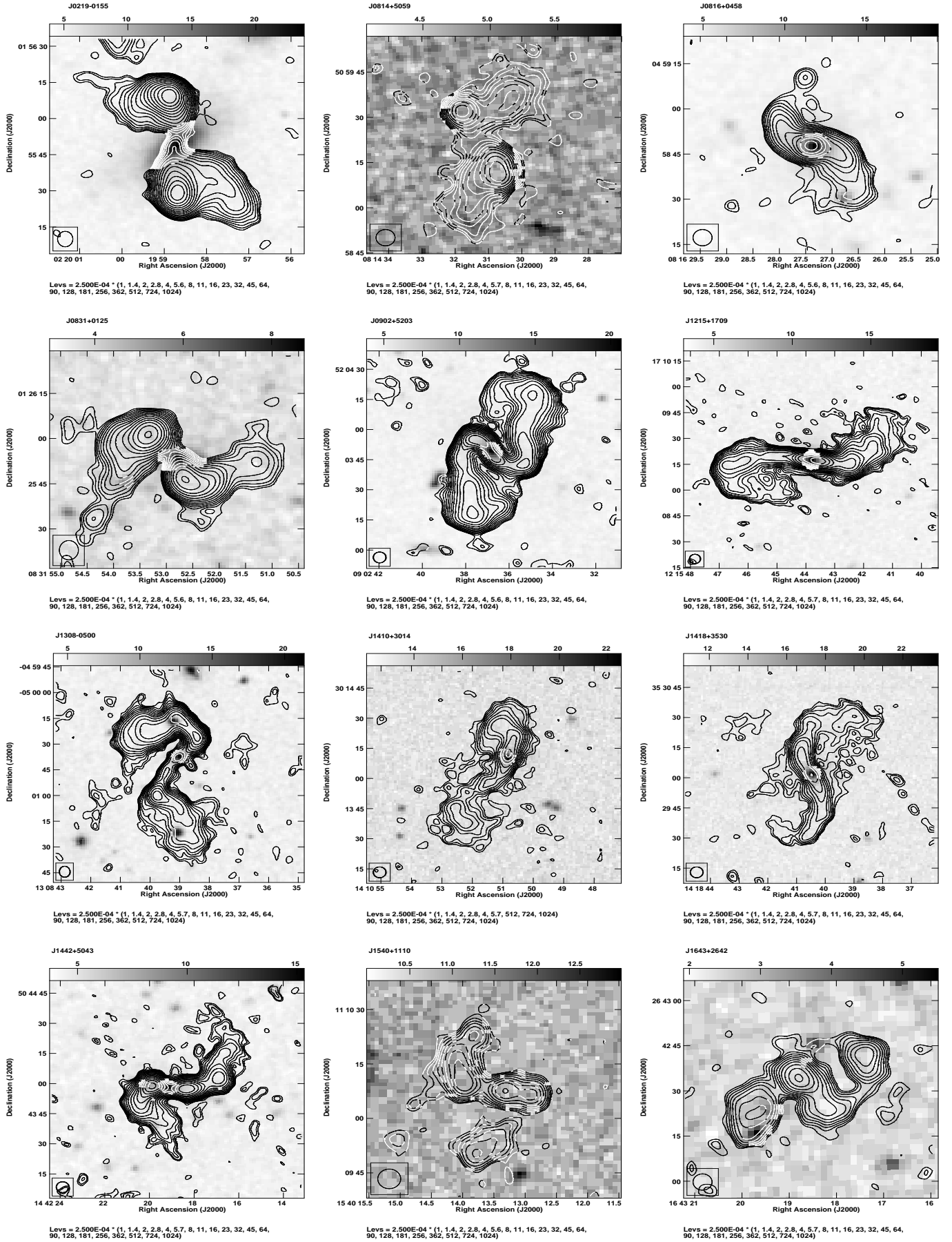


Figure 3. The FIRST image of a sample of 12 "Z"-shaped radio sources (contours) overlaid on the DSS2 red image (grey scale).

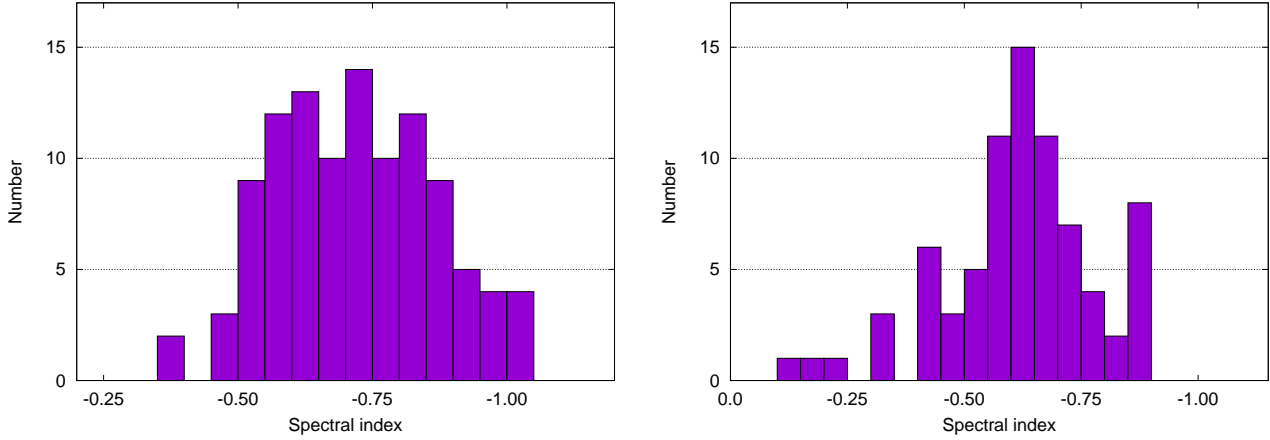


Figure 4. Histogram showing the spectral index distribution of radio galaxies presented in the current paper with "X" (left) and "Z" shapes (right).

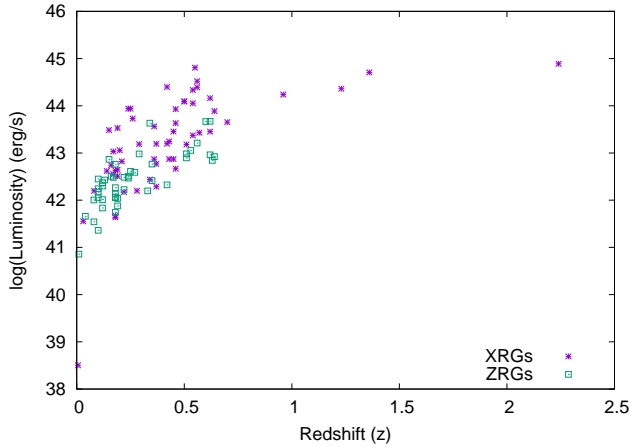


Figure 5. Distribution of radio luminosity (L_{rad}) with red shift (z) for XRGs and ZRGs.

3.3.2. Angle between the Major and Minor Axes

Figure 9 shows a histogram with the distribution of the angle between major and minor axes in XRGs. The angle between the intersection of two virtual lines with peak fluxes in each lobe of major and minor axes is used to measure the angle between two axes. Sources with one-sided wings are not included in the figure. Sources with diffused and nonlinear secondary lobes are also not included in the study to avoid error in angle measurement. Total 161 XRGs are used in the figure. Majority of the sources (63%) have the angle in the range of (70 – 90) degrees. The histogram shows a peak in the number of radio galaxies at 75 degrees.

3.4. Properties of the ZRGs

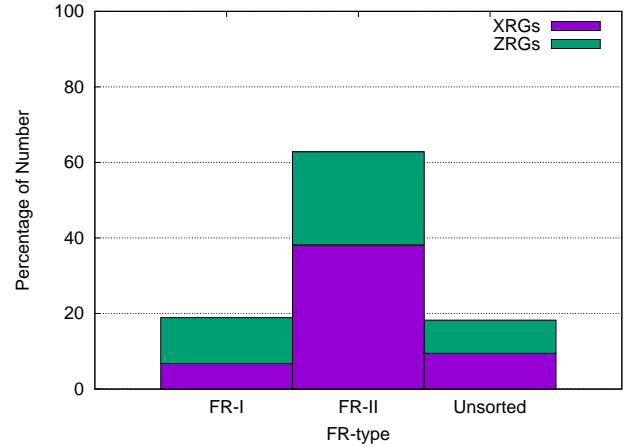


Figure 6. Histogram showing the number of FR I and FR II sources amongst the XRGs and ZRGs reported in the present paper.

Out of 135 ZRGs presented in the current paper, 54% (36) are FR II radio galaxies and 27% (73) are FR I radio galaxies. For 26 ZRGs, the jet morphology is complex and could not be classified.

3.4.1. The Angular Size

In Figure 10, the distribution of the angular size of primary jets in ZRGs is shown. Here we have measured the angular size of the primary jet in between the two oppositely directed secondary wings. The angular sizes depend on the lowest contour of the image. For uniformity, we have started contours from 0.25 mJy. The angular size is determined by the task 'tvdist' in AIPS.

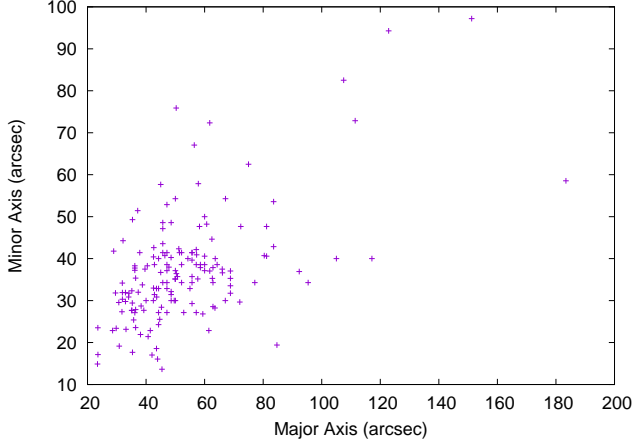


Figure 7. The distribution of the size of major and minor axes of the discovered radio galaxies with an X-like shape.

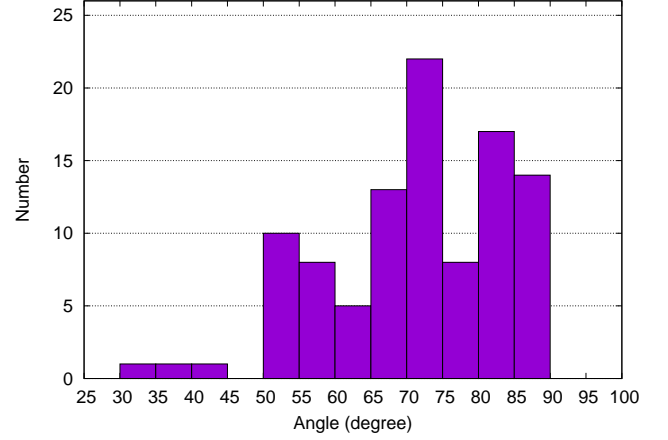


Figure 9. Histogram showing the distribution of angle between major and minor axes in "X"-shaped sources.

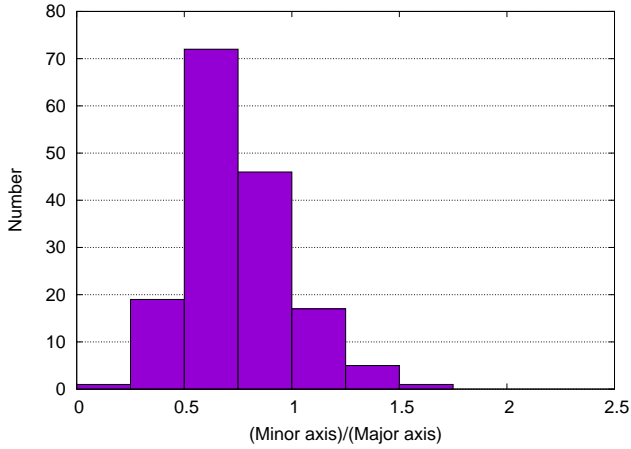


Figure 8. Histogram showing the distribution of size between major and minor axis in 'X' shaped sources.

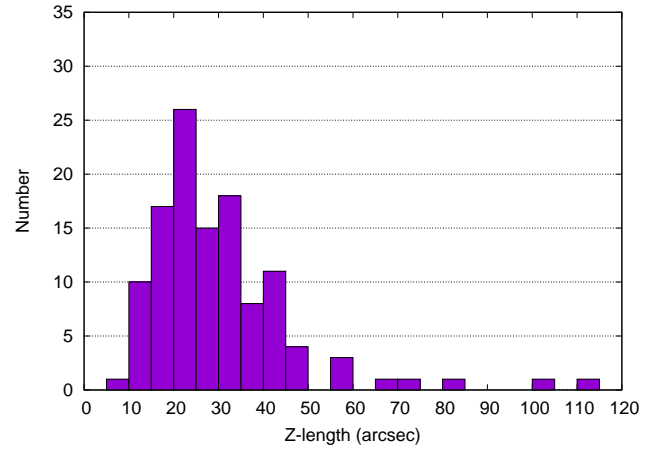


Figure 10. Histogram showing the distribution of the angular size of "Z"-shaped sources.

For most of the sources, the angular size of primary jets is less than 1 arcmin. The histogram shows a sharp peak near 20 arcsec. There are only two sources with a primary jet angular size of more than 90 arcsec. J1417+0812 has a primary jet angular size of 113 arcsec and J1303+0339 has an angular size of 104 arcsec. The ZRG with the smallest primary jet angular size is J2137–0811 (9 arcsec).

Amongst the sources with known redshift, the source with the highest primary jet linear size is J1319+0502 (1.41 Mpc). J1303+0339 and J1536+2357 have a primary jet linear sizes of 0.47 and 0.44 Mpc, respectively. J1140+1743 is the smallest source with the primary jet linear size of 5.85 kpc. The primary jet linear size of J0219+0155 is 37.8 kpc.

4. DISCUSSION

Out of a total of 161 XRGs and 135 ZRGs, redshifts are known for 72 and 63, respectively. Amongst the XRGs, $0 < z < 0.5$ for 53 sources and $z > 0.5$ for 19 sources. J1124+4325 showed the highest redshift with $z = 2.245$ (Richards et al. 2009). Spectroscopically, J1124+4325 is classified as a quasar (Xu & Han 2014). J1333+0219 and J0750+1144 showed redshifts of $z = 1.228$ (Nilsson 1998) and $z = 0.955$ (Richards et al. 2009), respectively. Amongst the ZRGs, $0 < z < 0.5$ for 53 sources and $z > 0.5$ for 10 sources. Amongst the ZRGs, J1319+0502 has the highest redshift at $z = 1.285$ (Richards et al. 2009). J1124+4325 and

J1319+0502 are the farthest known XRG and ZRG, respectively. Previously, J0229+132 ($z = 2.065$) was the farthest X-shaped radio source candidate with its large core dominance (Marecki et al. 2006). The highest redshift XRG in Cheung (2007) is J1206+3812 ($z = 0.838$). From the optical spectroscopy of X-shaped and Z-shaped sources reported earlier, it is found that a good fraction of the sources are quasars (Cheung 2007). Since number density of quasars peak at $z \sim 1 - 2$ (Boyle et al. 2000), we expect a good number of XRGs and ZRGs in these redshifts but since minor jets in faint sources (which are often diffused) are not detectable for many of the sources, we are missing many of the XRGs and ZRGs with $z > 1$.

For the XRG J0057–0123, two supernovae are found inside the radio map. SN 2010jo and SN 2007nq (Hakobyan et al. 2012) are located at 11.7 and 21.6 arcsec far from the center of the galaxy at one of the major lobes of the galaxy.

All the XRGs, with flux densities > 2 Jy, are FR II radio galaxies. Amongst XRGs, J1001+2847 is the brightest radio galaxy with flux density $F_{1400} = 5589$ mJy. J1001+2847 is a Seyfert galaxy (Véron-Cetty & Véron 2006). J0057–0123 ($F_{1400} = 5384$ mJy), J0655+5408 ($F_{1400} = 3727$ mJy), J1422+1935 ($F_{1400} = 3659$ mJy), J0950+1420 ($F_{1400} = 3639$ mJy), J1617+3222 ($F_{1400} = 3222$ mJy), and J1235+2120 ($F_{1400} = 2013$ mJy) have flux densities more than 2 Jy. Only one ZRG has a flux density greater than 1 Jy. J1140+1743 is the brightest ZRG with flux density 1154 mJy.

Though the present paper, along with C07 and Y19, report the discovery of a large number of XRGs and ZRGs from the FIRST survey, it should be remembered that, due to high resolution in the FIRST image and the absence of antennas with shorter baseline, a large number of XRGs and ZRGs with larger sizes and diffused emission will be missed.

As mentioned earlier, the wings in XRGs and ZRGs may be significantly shortened due to projection effects. The flux-density asymmetry between two sides of the wings, as found in some XRGs, may indicate that the wings are close to our line of sight and flux-density asymmetry is due to Doppler boosting. Some of the 26 sources with one-sided wing may be an extreme example of Doppler boosting.

We have identified 161 XRGs and 135 ZRGs, making the ratio of XRGs to ZRGs equal to 1.2. Earlier, Saripalli & Roberts (2018) pointed out using a sample of Cheung (2007) that the ratio of XRG to ZRG in their sample is ~ 2 . The current paper detected more ZRGs compared to Cheung (2007) due to the fact that ZRGs are statistically fainter than XRGs (see Section 3.1) and Cheung (2007) missed many of the ZRGs because of its dynamic range specific selection criterion. Saripalli & Roberts (2018) also pointed out that their sample has only one FR I sources (2.7%) out of 37 XRGs. Again, the present paper detected

more FR I sources than that reported in Saripalli & Roberts (2018) because FR I sources are statistically fainter than FR II sources and the present paper did not make any restrictions with respect to the dynamic range filtering out relatively fainter sources. The present paper shows that though most of XRGs are still FR II in the present sample (70%) FR I XRG sources are also not negligible (13%) contrary to the findings of Saripalli & Roberts (2018).

A total of 127 sources, i.e. 43% sources in our sample are inversion symmetric. Out of the 127 sources, 58 XRGs and 69 ZRGs are symmetric. The inversion symmetric structure hints at a host-related cause for the formation of wings.

To explain the nature of XRGs, the backflow of plasma is one of the widely accepted models. The buoyancy-driven backflow cannot propagate faster than the external sound speed (Leahy & Parma 1992) and so the wings produced by the buoyancy forces are not expected to be longer than the main radio lobes, which are known to advance supersonically. We have found seven sources where wings are longer than the primary axes. Saripalli & Roberts (2018) also found two such sources within their sample of 87 sources. So, for some of the XRGs, backflow may still occur but it is not the only reason for all of the XRGs (especially for sources with longer wings). But it is still possible that the alignment effect plays a roll in the primary jets for which it looks shorter than the secondary jets.

Multifrequency high-resolution observation of these sources is encouraged to confirm the nature of these sources. Discovery of a large number of XRGs and ZRGs shows that these kinds of sources are not rare, and with a future deeper high-resolution survey, we expect to discover more such objects.

5. CONCLUSION

We have discovered a total of 296 radio sources with wings, out of which 161 are XRGs and 135 are ZRGs. This discovery helps to increase the number of known XRGs and ZRGs significantly. Optical/IR counterparts of most of the XRGs and ZRGs are identified. As expected, most of the XRGs and ZRGs show a steep spectral index between 150 MHz and 1400 MHz. Most of the XRGs are FR II radio galaxies. The average value of luminosities for XRGs is found to be higher than that of ZRGs.

We thank the anonymous reviewer whose suggestion help to improve the quality of the paper. This research has made use of the NASA/IPAC Extra-galactic Database (NED), which is operated by the Jet Propulsion Laboratory, California Institute of Technology, under contract with the National Aeronautics and Space Administration. T.K.S. and S.M. want to acknowledge funding from Rashtriya Uchcharat Shiksha Abhijan 2.0.

REFERENCES

- Abell, G. O. 1958, ApJS, 3, 211
 Abell, G. O., Corwin H. G. Jr., & Olowin, R. P. 1989, ApJS, 70, 1
 Aghanim, N., Akrami, Y., Ashdown, M., et al. 2018, astro-ph:1807.06209

- Agüeros, M. A., Ivezić, Ž., Covey, K. R., et al. 2005, *The Astronomical Journal*, 130, 1022
- Baldwin, J. E., Boysen, R. C., Hales, S. E. G., et al. 1985, *MNRAS*, 217, 717
- Becker, R. H., White, R. L., & Helfand, D. J. 1995, *ApJ*, 450, 559
- Benn, C. R., Gruff, G., Vigotti, M., & Wall, J. V. 1982, *MNRAS*, 200, 747
- Benn, C. R., Grueff, G., Vigotti, M., & Wall, J. V. 1988, *MNRAS*, 230, 1
- Bennett, A. S. 1962, *MmRAS*, 68, 163
- Bhukta, N., Pal, S., Mondal, S. 2020, *MNRAS*, submitted, astro-ph: 2006.07219
- Bolton, J., Gardner, F., & Mackey, M. 1964, *Australian J. Phys.*, 17, 340
- Boyle, B. J., Shanks, T., Croom, S. M., Smith, R. J., Miller, L., Loaring, N., & Heymans, C. 2000, *MNRAS*, 317, 1014
- Brand, K., Rawlings, S., Hill, G. J., et al. 2003, *MNRAS*, 344, 283
- Brand, K., Rawlings, S., Hill, G. J., & Tufts, J. R. 2005, *MNRAS*, 357, 1231
- Capak, P. L., Teplitz, H. I., Brooke, T. Y., Laher, R., Science Center, Spitzer 2013, AAS Meeting, 221, id.340.06
- Capetti, A., Zamfir, S., Rossi, P., et al. 2002, *A&A*, 394, 39
- Caswell, J. L., & Crowther, J. H. 1969, *MmRAS*, 145, 181
- Cheung, C. C., 2007, *ApJ*, 133, 2097
- Chung, S. M., Eisenhardt, P. R., Gonzalez, A. H., et al. 2011, *ApJ*, 743, 10
- Cohen, A. S., Lane, W. M., Cotton, W. D., et al. 2007, *AJ*, 134, 1245
- Colla, G., Fanti, C., Ficarra, A., et al. 1970, *A&AS*, 1, 281
- Colla, G., Fanti, C., Fanti, R., et al. 1972, *A&AS*, 7, 1
- Colla, G., Fanti, C., Fanti, R., et al. 1973, *A&AS*, 11, 291
- Condon, J. J., Cotton, W. D., Greisen, E. W., et al. 1998, *AJ*, 115, 1693
- Dennett-Thorpe, J., Scheuer, P. A. G., Laing, R. A., et al. 2002, *MNRAS*, 330, 609
- Douglas, J. N., Bash, F. N., Bozyan, F. A., Torrence G. W., & Wolfe, C. 1996, *AJ*, 111, 1945
- Dreyer, J. L. E. 1888, *MmRAS*, 49, 1
- Edge, D. O., Shakeshaft, J. R., McAdam, W. B., Baldwin, J. E., & Archer, S. 1959, *MmRAS*, 68, 37
- Ekers, R. D., Fanti, R., Lari, C., & Parma, P. 1978, *Nature*, 276, 588
- Ennis, D. J., Neugebauer, G., & Werner, M. 1982, *Astrophys. J.* 262, 460
- Falco, E. E., Kurtz, M. J., Geller, M. J., et al. 1999, *PASP*, 111, 438
- Fanaroff, B.L., & Riley, J. M. 1974, *MNRAS*, 167, 31P
- Fanti, C., Fanti, R., Ficarra, A., & Padrielli, L. 1974, *A&AS*, 18, 147
- Ficarra, A., Grueff, G., & Tomassetti, G. 1985, *A&A*, 59, 255
- Gopal-Krishna & Wiita, P. J. 2000, *A&A*, 363, 507
- Goss, W. M., Pariiskii, Y. N., Soboleva, N. S., et al. 1992, *Soviet Astronomy*, 36, 343
- Gower, J. F. R., Scott, P. F., & Wills, D. 1967, *MmRAS*, 71, 49
- Gregory, P. C., & Condon, J. J. 1991, *ApJS*, 75, 1011
- Griffith, M. R., Wright, A. E., Burke, B. F., & Ekers, R. D. 1994, *ApJS*, 90, 179
- Gunn, J. E., Walter, A. S., Edward, J. M., et al. 2006, *AJ*, 131, 2332
- Hakobyan, A. A., Adibekyan, V. Zh., Aramyan, L. S., et al., 2012, *A&A*, 544, 81
- Hales, S. E. G., Baldwin, J. E., & Warner, P. J. 1988, *MNRAS*, 234, 919
- Hales, S. E. G., Masson, C. R., Warner, P. J., & Baldwin, J. E. 1990, *MNRAS*, 246, 256
- Hales, S. E. G., Baldwin, J. E., & Warner, P. J. 1993a, *MNRAS*, 263, 25
- Hales, S. E. G., Masson, C. R., Warner, P. J., Baldwin, J. E., & Green, D. A. 1993b, *MNRAS*, 262, 1057
- Hales, S. E. G., Mayer, C. J., Warner, P. J., & Baldwin, J. E. 1991, *MNRAS*, 251, 46
- Hao, J., McKay, T. A., Koester, B. P et al. 2010, *ApJS*, 191, 254
- Heeschen, D. S. 1966, *ApJ*, 146, 517H
- Hewitt, A., Burbidge, G., 1991, *ApJS*, 75, 297
- Ho, L. C., Kim, M., 2009, *ApJS*, 184, 398
- Intema, H. T., van Weeren, R. J., Röttgering, H. J. A., & Lal, D. V. 2011, *A&A*, 535, A38
- Intema, H. T., Jagannathan, P., Mooley, K. P., & Frail, D. A. 2017, *A&A*, 598, 78
- Jones, D. H., Read, M. A., Saunderset, W., et al. 2009, *MNRAS*, 399, 683
- Kotanyi, C. 1990, *Mexicana Astron. Astrof.*, 21, 173
- Kenderdine, S., Ryle, M. S., & Pooley, G. G., 1966, *MNRAS*, 134, 189
- Koester, B. P, McKay, T. A., Annis, J., et al. 2007, *ApJ*, 660, 239
- Kollgaard, R. I., Brinkmann, W., Chester, M. M., et al. 1994, *ApJS*, 93, 145
- Kunert, M., Marecki, A., Spencer, R. E., Kus, A. J., & Niezgoda, J. 2002, *A&A*, 391, 47
- Kuźmicz, A., Jamrozy, M., Bronarska, K., Janda-Boczar, K., & Saikia, D. J. 2018 *ApJS*, 238, 9
- Leahy, J. P., & Williams, A. G. 1984, *MNRAS*, 210, 929
- Leahy, J. P., & Parma, P. 1992, *Proc. 7th. I.A.P. Meeting: Extragalactic Radio Sources. From Beams to Jets*, 307
- Machalski, J., 1998, *A&AS*, 128, 153
- Mack, K. H., Gregorini, L., Parma, P., & Klein, U. 1994, *A&AS*, 103, 157
- Maddox, S. J., Efstathiou, G., Sutherland, W. J., & Loveday, J. 1990, *MNRAS*, 243, 692
- Marecki, A., Thomasson, P., Mack, K.-H., & Kunert-Bajraszewska, M. 2006, *A&A*, 448, 479
- McGee, R. X., & Newton, L. M. 1972, *Aust. J. Phys.* 25, 619

- McGee, R. X., Newton, L. M., & Butler, P. W. 1976, *Aust. J. Phys.*, 29, 329
- McGilchrist, M. M., Baldwin, J. E., Riley, J. M., et al. 1990, *MNRAS*, 246, 110
- Merritt, D., & Ekers, R. D. 2002, *Science*, 297, 1310
- Milne, D. K., Caswell, J. L., & Haynes, R. F. 1980, *MNRAS*, 191, 469
- Missaglia, V., Massaro, F., Capetti, A., et al. 2019, *A&A*, 626, A8
- Nilsson, K., Valtonen, M. J., Kotilainen, J., & Jaakkola, T. 1993, *ApJ*, 413, 453
- Nilsson, K. 1998, *A&AS*, 132, 31
- O’Dea, C. P., & Owen, F. N. 1987, *AJ*, 316, 95
- Peacock, J. A. 1983, *MNRAS*, 202, 615
- Pearson, T. 1975, *MNRAS*, 171, 475
- Pearson, T., & Kus, A. J. 1978, *MNRAS*, 182, 273
- Pilkington, J. D. H., & Scott, J. F. 1965, *MNRAS*, 69, 183
- Pooley, G. G. 1969, *MNRAS*, 144, 101
- Pooley, G. G., & Kenderdine, S. 1968, *MNRAS*, 139, 529
- Proctor, D. D. 2011, *ApJS*, 194, 31
- Rebull, L. M., Koenig, X. P., Padgett, D. L. et al. 2011, *ApJS*, 196, 19
- Richards, G. T., Myers A. D., Gray, A. G., et al. 2009, *ApJS*, 180, 67
- Riley, J. M. 1972, *MNRAS*, 157, 349
- Rottmann, H. 2001, PhD thesis, Univ. Bonn
- Rykoff, E. S., Koester, B. P., Rozo, E., et al., 2012, *ApJ*, 746, 178
- Saripalli, L., & Roberts, D. H. 2018, *ApJ*, 852, 21
- Sasmal, T. K., Pal, S., Bera, S., Mondal, S. 2020, *MNRAS*, submitted
- Sánchez, A. J., Aguerri, J. A. L., Muñoz-Tuñón, C., & Huertas-Company, M. 2011, *ApJ*, 735, 15
- Schuch, N. 1981, *MNRAS*, 196, 695
- Shectman, S. A., Landy, S. D., Oemler, A., et al. 1996, *ApJ*, 470, 172
- Skrutskie, M. F., Cutri, R. M., Stiening, R., et al. 2006, *AJ*, 131, 1163
- Slee, O. 1995, *Australian J. Phys.*, 48, 143
- Smirnov, N. 1948, *Annals of Mathematical Statistics*, 19, 279
- Tiwari, P. 2019, *Research in Astron. Astrophys.*, accepted, arXiv:1609.01308v3.
- Ubachukwu, A. A., & Onuora, L. I. 1993, *Ap&SS*, 209, 169
- Véron-Cetty, M. P., Véron, P. 2006, *A&A*, 455, 773
- Vessey, S. J., & Green, D. A. 1998, *MNRAS*, 294, 607
- Vorontsov-Vel’Yaminov, B. A., & Arkhipova V. P. 1962, *Morphological Trudy Gos. Astron. Inst. Shternberga*, 1
- Waggett, P. 1977, *MNRAS*, 181, 547
- Waldram, E. M., Yates, J. A., Riley, J. M., & Warner, P. J. 1996, *MNRAS*, 282, 779
- Wegner, G., Colless, M., Baggley, G., et al. 1996, *ApJS*, 106, 1
- Wen, Z. L., Han, J. L., & Liu, F. S. 2010, *ApJS*, 187, 272
- White, R. L., & Becker, R. H. 1992, *ApJS*, 79, 331
- White, R. L., Becker, R. H., Helfand, D. J., & Gregg, M. D. 1996, *ApJ*, 475, 479
- Williams, P. J. S., & Bridle, A. H. 1967, *The Observatory*, 87, 280
- Willson, M. 1970, *MNRAS*, 151, 1
- Xu, J., & Han, J. L. 2014, *MNRAS*, 442, 3329
- Yang, X., Joshi, R., Gopal-Krishna 2019, *ApJS*, 245, 17

Table 1. Candidate X-Shaped Radio Sources

Catalog Number	Name	R.A. (J2000.0)	Decl. (J2000.0)	Ref.	Redshift (z)	F_{1400} (mJy)	F_{150} (mJy)	α_{150}^{1400}	Linear Size (kpc)	L (ergs^{-1}) ($\times 10^{42}$)	Other Catalogs
1	J0017-0149	00 17 32.20	-01 49 25.9	GALEXMSC	—	91	—	—	—	—	1, 2, 8
2	J0022-0807	00 22 55.64	-08 07 52.4	SDSS	0.44	98	—	—	796	—	1
3	J0023-0915	00 23 25.26	-09 15 38.2	SDSS	—	117	—	—	—	—	1
4	J0057-0123	00 57 34.92	-01 23 27.9	SDSS	0.04	5348	—	—	137	—	2, 3, 8, 9, 10, 11, 14, 24, 29
5	J0110-0924	01 10 34.36	-09 24 45.2	EE	—	135	—	—	—	—	1, 2, 8, 10
6	J0112-0804	01 12 42.41	-08 04 02.4	EE	—	365	—	—	—	—	1, 2, 8, 10
7	J0139+0131	01 39 57.25	+01 31 46.2	GALEXASC	0.26 ³⁰	1312	4750	-0.58	415	53.65	1, 2, 4, 8, 9, 10, 11, 12
8	J0144+1212	01 44 36.38	+12 12 54.8	EE	—	11	38	-0.56	—	—	1
9	J0145-0941	01 45 03.87	-09 41 16.6	SSTSL2	—	90	—	—	—	—	—
10	J0152-0759	01 52 39.32	-07 59 13.8	SDSS	0.41	79	—	—	772	—	—
11 ^a	J0212-0450	02 12 16.55	-04 50 38.8	EE	—	157	—	—	—	—	8
12	J0335-0719	03 35 48.23	-07 19 12.5	EE	—	86	—	—	—	—	1, 2
13	J0354-0522	03 54 04.69	-05 22 08.9	EE	—	608	—	—	—	—	1, 2, 4, 8, 9, 10
14	J0355-0553	03 55 24.70	-05 53 19.8	EE	—	80	—	—	—	—	1
15	J0654+5814	06 54 22.91	+58 14 26.0	EE	—	95	621	-0.84	—	—	—
16	J0655+5408	06 55 14.73	+54 08 57.2	GALEXASC	0.24 ³¹	3727	31666	-0.96	320	86.98	1, 2, 3, 10, 12
17	J0703+6014	07 03 11.18	+60 14 23.1	2MASX	—	55	154	-0.46	—	—	1
18	J0709+5716	07 09 58.26	+57 16 51.6	EE	—	271	1660	-0.81	—	—	1, 2, 6, 10, 12
19	J0712+5430	07 12 45.08	+54 30 10.8	EE	—	381	2406	-0.82	—	—	1, 2, 6, 10, 12
20	J0719+5519	07 19 36.64	+55 19 42.8	EE	—	61	424	-0.87	—	—	1
21	J0721+3551	07 21 29.03	+35 51 38.2	SDSS	—	503	4799	-1.01	—	—	—
22	J0723+3323	07 23 59.55	+33 23 20.2	EE	—	148	525	-0.57	—	—	1, 2, 6, 12, 20
23 ^a	J0742+3339	07 42 59.47	+33 39 52.7	SDSS	0.64	334*	2729	-0.94	1214	77.05	—
24	J0743+1733	07 43 24.28	+17 33 41.3	EE	—	423	2494	-0.79	—	—	1, 2, 10, 12
25	J0747+2202	07 47 36.74	+22 02 15.9	SDSS	0.46	44	301	-0.86	606	4.65	1
26	J0748+2324	07 48 45.10	+23 24 45.8	SDSS	0.19	515	3238	-0.82	260	33.87	—
27	J0749+2007	07 49 19.08	+20 07 53.7	SDSS	0.37	139	960	-0.86	518	1.94	1, 2, 10, 12
28	J0750+1144	07 50 25.95	+11 44 52.0	SDSS	0.96	289	1846	-0.83	1512	172.51	15
29	J0758+4406	07 58 08.43	+44 06 17.0	EE	—	31	68	-0.35	—	—	1
30	J0758+1946	07 58 19.52	+19 46 56.5	SDSS	—	51	421	-0.94	—	—	1
31	J0758+1020	07 58 26.24	+10 20 18.6	SDSS	0.37	213	977	-0.68	447	15.63	1, 2, 12
32	J0802+6353	08 02 02.34	+63 53 03.3	LQAC	0.47	1052	—	—	1386	—	2, 6, 10, 12
33 ^a	J0804+4659	08 04 53.99	+46 59 57.0	EE	—	52	—	—	—	—	1
34	J0811+2954	08 11 11.85	+29 54 53.6	EE	—	162	1550	-1.01	—	—	1, 2, 12, 20
35	J0817+2951	08 17 03.62	+29 51 47.1	TONS08w	0.37 ³²	93	686	-0.89	316	5.88	1, 10
36	J0823+0335	08 23 16.90	+03 35 36.5	EE	—	90	214	-0.39	—	—	1
37	J0825+4623	08 25 24.05	+46 23 33.8	EE	—	38	148	-0.61	—	—	—
38	J0827+3748	08 27 05.80	+37 48 42.2	EE	0.21	379	3644	-1.01	446	6.65	1, 2, 4, 10, 12, 20
39	J0828+3057	08 28 03.00	+30 57 42.8	SDSS	0.36	102	460	-0.67	440	7.39	1, 2, 12, 20
40 ^a	J0830+3510	08 30 36.26	+35 10 59.2	SDSS	—	76	—	—	—	—	1, 2
41	J0840+6413	08 40 25.47	+64 13 17.7	EE	—	30	213	-0.88	—	—	1
42	J0849+0949	08 49 40.02	+09 49 21.2	SDSS	0.36	575	3532	-0.81	816	36.52	2, 4, 8, 9, 10, 11, 15
43 ^a	J0857-0339	08 57 11.73	-03 39 41.0	EE	0.17	1103	—	—	405	—	1, 2, 4, 8, 9, 10, 11, 15
44	J0858+5740	08 58 03.85	+57 40 13.8	SDSS	0.45	61	253	-0.64	427	7.45	1, 6, 12
45	J0906+1646	09 06 32.53	+16 46 05.6	SDSS	0.41	1616	—	—	818	—	3
46	J0914+6121	09 14 00.60	+61 21 11.6	EE	—	22	110	-0.72	—	—	—
47	J0917+4259	09 17 35.04	+42 59 07.6	SDSS	—	81	346	-0.65	—	—	1
48	J0931-0540	09 31 41.67	-05 40 48.0	EE	—	10	—	—	—	—	1
49	J0932+1610	09 32 43.96	+16 10 53.1	EE	—	273*	—	—	—	—	1, 2
50	J0933-0507	09 33 37.48	-05 07 18.8	EE	—	90	—	—	—	—	—
51	J0938+4520	09 38 34.68	+45 20 23.7	SDSS	0.45	258	1286	-0.72	906	28.51	1, 2, 6, 10, 12, 21
52	J0941+3853	09 41 04.00	+38 53 50.9	SDSS	0.62	682	4176	-0.81	1325	144.90	1, 2, 4, 10, 20
53	J0950+1420	09 50 10.79	+14 20 00.6	SDSS	0.55	3639	18298	-0.72	984	640.99	1, 2, 3, 11, 15
54 ^a	J1001+2847	10 01 49.52	+28 47 08.9	SDSS	0.18	5589	—	—	561	—	2, 4, 10, 11, 20
55	J1021+4425	10 21 16.98	+44 25 39.8	EE	—	94	—	—	—	—	—
56	J1022+5213	10 22 12.66	+52 13 42.4	EE	—	151	1385	-0.99	—	—	1, 2, 7, 10, 12
57	J1023+4334	10 23 05.05	+43 34 33.2	EE	—	145	816	-0.77	—	—	—
58	J1031+5225	10 31 43.51	+52 25 35.1	SDSS	0.17	920	4846	-0.74	275	10.77	1, 2, 4, 10
59 ^a	J1032+2730	10 32 57.60	+27 30 15.1	SDSS	—	72	262	-0.58	—	—	1, 16

Table 1. Candidate X-Shaped Radio Sources

Catalog Number	Name	R.A. (J2000.0)	Decl. (J2000.0)	Ref.	Redshift (z)	F_{1400} (mJy)	F_{150} (mJy)	α_{150}^{1400}	Linear Size (kpc)	L (ergs s^{-1}) ($\times 10^{42}$)	Other Catalogs
60	J1049+5711	10 49 06.22	+57 11 53.0	EE	—	16	54	-0.54	—	—	1, 7
61	J1050+3240	10 50 11.17	+32 40 24.8	SDSS	—	33	119	-0.56	—	—	1, 7
62	J1107+5716	11 07 38.59	+57 16 00.4	EE	—	13	—	—	—	—	1
63	J1115+4314	11 15 21.25	+43 14 37.8	SDSS	0.46	350	1611	-0.68	540	42.78	6
64	J1122+0046	11 22 00.98	+00 46 31.5	EE	—	293	910	-0.51	—	—	1, 8, 10
65	J1124+4325	11 24 12.23	+43 25 50.0	SDSS	2.24	168	698	-0.64	3347	775.75	1, 2, 6, 10, 15
66	J1124+1717	11 24 57.40	+17 17 44.7	SDSS	0.14	12	—	—	113	—	1
67	J1130+3434	11 30 05.74	+34 34 28.8	EE	—	205	1315	-0.83	—	—	1, 7, 20
68	J1134+3835	11 34 03.87	+38 35 52.4	SDSS	0.50	324	—	—	852	—	1, 2, 12, 20
69	J1136-0329	11 36 01.40	-03 29 09.5	EE	—	292	—	—	—	—	1, 2, 10
70	J1138+1845	11 38 52.17	+18 45 33.2	SDSS	0.18	22	74	-0.54	172	0.43	1
71	J1141-0723	11 41 47.83	-07 23 24.7	APMUKS	—	114	—	—	—	—	1
72	J1142+5832	11 42 23.84	+58 32 01.5	EE	—	160	—	—	—	—	—
73	J1144+1031	11 44 20.33	+10 31 35.3	SDSS	0.28	38	160	-0.64	274	1.58	1
74	J1149+2554	11 49 08.01	+25 54 38.7	EE	—	62	410	-0.84	—	—	—
75	J1149+4618	11 49 50.67	+46 18 50.6	SDSS	0.62	129	776	-0.80	1025	28.40	1, 2, 6, 12, 21
76	J1150+3622	11 50 50.16	+36 22 03.7	SDSS	0.14	540	3435	-0.83	209	4.16	1, 2, 4, 10, 12, 20
77	J1155-0646	11 55 52.78	-06 46 37.9	EE	—	36	—	—	—	—	1
78	J1157+0845	11 57 54.33	+08 45 01.4	SDSS	0.43	176	873	-0.72	754	17.58	1, 2, 10
79	J1201+2520	12 01 24.72	+25 20 23.7	SDSS	0.50	857	4160	-0.71	977	123.97	1, 2, 4, 20
80	J1210+3157	12 10 37.57	+31 57 06.0	SDSS	0.39	274	—	—	1019	—	2, 7
81	J1211+5717	12 11 22.96	+57 17 51.7	SDSS	—	220	1999	-0.99	—	—	1, 2, 6
82	J1213+1343	12 13 06.68	+13 43 17.8	SDSS	0.17	225	884	-0.61	229	3.56	13, 16
83	J1220+6053	12 20 04.90	+60 53 16.5	SDSS	0.34	32	100	-0.51	383	2.74	1
84	J1222-0638	12 22 48.91	-06 38 01.7	EE	—	95	—	—	—	—	1, 2
85	J1235+2120	12 35 26.66	+21 20 34.7	SDSS	0.42	2913	21017	-0.88	2117	249.94	2, 3, 9, 10, 11,
86	J1238+2752	12 38 26.08	+27 52 06.5	EE	—	72	268	-0.59	—	—	—
87	J1239+1706	12 39 04.34	+17 06 26.2	SDSS	—	44	272	-0.82	—	—	—
88	J1242+4244	12 42 37.96	+42 44 03.1	SDSS	—	277	1216	-0.66	—	—	4, 1
89	J1247+0807	12 47 55.91	+08 07 33.9	SDSS	0.43	68	288	-0.65	527	7.44	1
90	J1252-0120	12 52 30.70	-01 20 17.3	SDSS	0.36	269	—	—	612	—	1, 2, 8, 10
91 ^a	J1258+4435	12 58 00.87	+44 35 28.7	SDSS	—	960	—	—	—	—	15
92	J1300+2215	13 00 49.09	+22 15 47.4	SDSS	0.22	47	154	-0.53	298	1.48	1, 13
93	J1311-0234	13 11 34.09	-02 34 08.0	EE	—	381	—	—	—	—	—
94	J1311+4101	13 11 44.32	+41 01 58.3	EE	—	420	—	—	—	—	—
95	J1325+1535	13 25 43.66	+15 35 52.1	SDSS	—	69	512	-0.90	—	—	—
96	J1333+0219	13 33 45.13	+02 19 12.0	SDSS	1.23	200	930	-0.69	2249	230.13	1, 2, 9
97 ^a	J1336-0730	13 36 06.55	-07 30 25.5	APMUKS	—	70	—	—	—	—	1
98	J1336+3626	13 36 27.73	+36 26 27.3	EE	—	102	526	-0.73	—	—	1
99	J1338+3851	13 38 49.80	+38 51 11.7	EE	0.25	3461	23868	-0.86	363	87.07	1, 2, 3, 10, 12, 20
100	J1349+1858	13 49 06.04	+18 58 28.0	SDSS	0.19	189	839	-0.67	279	3.22	1, 2, 10, 12
101	J1354+5840	13 54 45.99	+58 40 00.7	SDSS	5.7E-3	15	44	-0.48	3	3.19E-4	1, 14, 15, 19
102 ^a	J1358+1203	13 58 59.01	+12 03 58.7	EE	—	43	184	-0.65	—	—	1
103	J1400+2719	14 00 08.00	+27 19 14.1	EE	0.16	534	2738	-0.73	320	5.51	1, 2, 4, 20
104 ^a	J1403+3827	14 03 11.75	+38 27 59.4	SDSS	0.54	674	3419	-0.73	1437	112.94	4
105	J1407+5131	14 07 24.20	+51 31 24.4	EE	—	420	—	—	—	—	—
106	J1412+1739	14 12 17.00	+17 39 48.0	EE	—	23	—	—	—	—	1
107	J1412+5839	14 12 47.81	+58 39 34.7	EE	—	40	235	-0.79	—	—	1
108	J1417+4051	14 17 58.37	+40 51 53.3	SDSS	—	252	1487	-0.79	—	—	—
109	J1418+2323	14 18 32.78	+23 23 34.7	EE	—	22	110	-0.72	—	—	—
110	J1419+2303	14 19 42.59	+23 03 27.6	EE	—	24	208	-0.97	—	—	—
111	J1420+5122	14 20 29.66	+51 22 33.9	SDSS	0.70	148	773	-0.74	771	44.98	16
112	J1422+5022	14 22 25.25	+50 22 13.3	SDSS	0.18	22	69	-0.51	131	0.47	1, 14
113	J1422+1935	14 22 58.76	+19 35 45.8	EE	—	3659	—	—	—	—	—
114 ^a	J1424+0025	14 24 19.98	+00 25 36.5	SDSS	—	159	714	-0.67	—	—	1, 2, 8, 10
115 ^a	J1440+6035	14 40 48.22	+60 35 46.0	SDSS	—	166	849	-0.73	—	—	1, 6
116	J1443+1440	14 43 00.08	+14 40 17.0	EE	—	66	276	-0.64	—	—	12
117 ^a	J1454+0959	14 54 05.82	+09 59 52.6	SDSS	—	100	329	-0.53	—	—	12
118 ^a	J1504+5749	15 04 08.06	+57 49 22.6	SDSS	—	94	—	—	—	—	1
119 ^a	J1506+2027	15 06 19.14	+20 27 40.8	SDSS	—	293	2353	-0.93	—	—	12
120	J1516+3205	15 16 47.11	+32 05 14.7	SDSS	0.54	112	389	-0.56	480	23.56	1, 2, 6, 12
121	J1519+5342	15 19 36.72	+53 42 55.4	SDSS	0.48	479	—	—	772	—	15

Table 1. Candidate X-Shaped Radio Sources

Catalog Number	Name	R.A. (J2000.0)	Decl. (J2000.0)	Ref.	Redshift (z)	F_{1400} (mJy)	F_{150} (mJy)	α_{150}^{1400}	Linear Size (kpc)	L (ergs^{-1}) ($\times 10^{42}$)	Other Catalogs
122	J1519-0408	15 19 49.79	-04 08 42.9	EE	—	231	—	—	—	—	2, 8, 10
123	J1523+1130	15 23 27.56	+11 30 23.9	SDSS	0.20	413	1258	-0.50	247	11.37	1, 2, 12, 15
124 ^a	J1523+2116	15 23 31.75	+21 16 56.8	SDSS	—	60	223	-0.59	—	—	1
125	J1537+3902	15 37 49.51	+39 02 37.6	SDSS	—	94	492	-0.74	—	—	21
126	J1539+5030	15 39 56.56	+50 30 08.7	EE	—	85	279	-0.53	—	—	1
127	J1553+2811	15 53 07.01	+28 11 24.7	EE	—	54	226	-0.64	—	—	1
128	J1553+2348	15 53 43.59	+23 48 25.4	SDSS	0.12	618	—	—	424	—	2, 4, 11, 12, 14, 15
129	J1558+3404	15 58 31.84	+34 04 44.0	SDSS	0.51	87	329	-0.60	556	15.17	1
130	J1605+1743	16 05 08.98	+17 43 47.6	SDSS	0.03	793	3092	-0.61	40	0.36	1, 2, 4, 11, 14, 19
131	J1607+1551	16 07 06.99	+15 51 33.9	SDSS	0.50	651	2044	-0.51	669	123.79	—
132	J1617+3222	16 17 42.53	+32 22 34.3	SDSS	0.15	2587	10002	-0.60	386	30.54	2, 3, 10, 11, 20
133	J1620+1736	16 20 21.82	+17 36 24.0	SDSS	0.56	1995	16503	-0.94	1148	330.25	2, 4, 11, 12, 15
134	J1626+4827	16 26 54.30	+48 27 39.1	SDSS	—	37	167	-0.67	—	—	1
135	J1628+1658	16 28 31.47	+16 58 33.3	SDSS	—	38	160	-0.64	—	—	1
136	J1633+3025	16 33 23.72	+30 25 00.4	SDSS	0.57	124	482	-0.61	565	26.93	20
137 ^a	J1635+3722	16 35 02.53	+37 22 14.7	SDSS	0.46	645	2630	-0.63	862	84.95	4
138	J1643+3729	16 43 06.16	+37 29 30.3	SDSS	0.56	1440	8535	-0.80	906	246.99	—
139	J1650+3455	16 50 26.81	+34 55 36.0	SDSS	0.19	216	788	-0.58	255	4.42	20
140	J1708+2435	17 08 46.13	+24 35 28.8	SDSS	1.36	369	2176	-0.79	2890	508.52	—
141	J1709+3425	17 09 39.15	+34 25 50.8	SDSS	0.08	646	3534	-0.76	113	1.58	4, 10, 11, 12
142	J1712+3857	17 12 11.13	+38 57 06.8	SDSS	—	192	724	-0.59	—	—	1
143 ^a	J1715+5420	17 15 39.44	+54 20 59.6	SDSS	0.18	320	2642	-0.94	229	4.24	1, 2, 4, 10, 12
144	J1719+6155	17 19 25.16	+61 55 33.9	EE	—	360	1989	-0.76	—	—	—
145	J1742+5917	17 42 43.67	+59 17 07.3	SDSS	—	1090	6030	-0.76	—	—	—
146	J1742+6145	17 42 51.59	+61 45 54.6	SDSS	0.54	1347	7048	-0.74	897	216.66	6
147	J2122+0001	21 22 17.10	+00 01 15.5	SDSS	0.42	157	722	-0.68	491	15.73	1, 12
148	J2123+1033	21 23 19.52	+10 33 26.0	SDSS	—	154	576	-0.59	—	—	1
149	J2153+0025	21 53 24.83	+00 25 25.7	EE	—	38	128	-0.54	—	—	1
150 ^a	J2213-0854	22 13 12.57	-08 54 34.1	EE	—	600	—	—	—	—	—
151	J2213-0544	22 13 35.87	-05 44 22.7	EE	—	32	—	—	—	—	1
152	J2215-0525	22 15 01.79	-05 25 17.5	2MASX	0.09 ³³	216	—	—	161	—	—
153	J2218+0012	22 18 30.16	+00 12 21.2	SDSS	0.29	412*	2763	-0.85	627	15.44	—
154	J2221-0326	22 21 29.54	-03 26 16.8	EE	0.36	83	—	—	475	—	1
155 ^a	J2243-0954	22 43 49.64	-09 54 07.7	SDSS	—	87	—	—	—	—	—
156	J2248-0449	22 48 30.44	-04 49 45.2	EE	—	43	—	—	—	—	1
157	J2249+0209	22 49 40.32	+02 09 28.4	EE	—	182	1894	-1.05	—	—	1, 2, 12
158	J2257-0603	22 57 50.82	-06 03 42.5	EE	—	46	—	—	—	—	1
159	J2301+1136	23 01 57.79	+11 36 46.2	EE	—	161	860	-0.75	—	—	1, 2, 10, 12
160	J2324+1438	23 24 32.09	+14 38 21.9	SDSS	0.04	116*	—	—	46	—	1, 2, 11, 29
161	J2351-0109	23 51 56.12	-01 09 13.4	SDSS	0.17	1624	—	—	223	—	1, 2, 4, 8, 9, 10, 11, 14

References— 1: NVSS (Condon et al. 1998); 2: VLA Low-Frequency Sky Survey (VLSS) (Cohen et al. 2007); 3: 3C (Bennett 1962; Edge et al. 1959); 4: 4C (Pilkington & Scott 1965; Gower et al. 1967; Caswell & Crowther 1969); 5: 5C (Kenderdine et al. 1966; Pooley & Kenderdine 1968; Pooley 1969; Willson 1970; Pearson 1975; Waggett 1977; Pearson & Kus 1978; Schuch 1981; Benn et al. 1982, 1988); 6: 6C (Baldwin et al. 1985; Hales et al. 1988, 1990, 1991, 1993a,b); 7: 7C (McGilchrist et al. 1990; Kollgaard et al. 1994; Waldram et al. 1996; Vessey & Green 1998); 8: Parkes-MIT-NRAO (PMN) (Griffith et al. 1994); 9: The Parkes catalogue of radio sources (PKS) (Bolton et al. 1964); 10: Texas Survey of Radio Sources (TXS) (Douglas et al. 1996); 11: Cul (Slee 1995); 12: 87GB (Gregory & Condon 1991); 13: Automatic Spectroscopic K-means-based classification (ASK) (Sánchez et al. 2011); 14: 2 Micron All Sky Survey Extended objects - Final Release (2MASX) (Skrutskie et al. 2006); 15: GALaxy Evolution eXplorer all-sky catalog (GALEXASC) (Agüeros et al. 2005); 16: Galaxy Evolution Explorer Medium-deep Sky Catalog (GALEXMSC) (Agüeros et al. 2005); 17: Gaussian Mixture Brightest Cluster Galaxy (GMBCG) (Hao et al. 2010); 18: Maximum likelihood redshift Brightest Cluster Galaxy (MaxBCG) (Koester et al. 2007); 19: New General Catalogue (NGC) (Dreyer 1888); 20: B2 (Colla et al. 1970, 1972, 1973; Fanti et al. 1974); 21: B3 (Ficarra et al. 1985); 22: RC (Goss et al. 1992); 23: WHL (Wen et al. 2010); 24: MGC (Vorontsov-Vel'Yaminov & Arkipova 1962); 25: Abell Clusters of Galaxies (ABELL) (Abell 1958; Abell et al. 1989); 26: Wide-field Infrared Survey Explorer (WISE) (Chung et al. 2011; Rebull et al. 2011); 27: WISE Blazar-like Radio-loud Sources (WB) (White & Becker 1992); 28: Automated Plate Measurement United Kingdom Schmidt (APMUKS) (Maddox et al. 1990); 29: Galaxy Identification Number (GIN) (Wegner et al. 1996); 30: Ho & Kim (2009); 31: Hewitt & Burbidge (1991); 32: Brand et al. (2005); 33: Jones et al. (2009); Spitzer Space Telescope Source List - version 4.2 (SSTSL2) (Capak et al. 2013); Las Campanas Redshift Survey (LCRS) (Shectman et al. 1996); Texas-Oxford NVSS Structure 08^h region (TONS08) (Brand et al. 2003); Texas-Oxford NVSS Structure 08^h region wider survey (TONS08w) (Brand et al. 2005)

Notes— ^a The source is present in Proctor (2011).

* The FIRST flux (at 1400 MHz) is used instead of the NVSS flux (at 1400 MHz).

Table 2. Candidate *S/Z*-Shaped Radio Sources

Catalog Number	Name	R.A. (J2000.0)	Decl. (J2000.0)	Ref.	Redshift (<i>z</i>)	F_{1400} (mJy)	F_{150} (mJy)	α_{150}^{1400}	Linear Size (kpc)	L (ergs^{-1}) ($\times 10^{42}$)	Other Catalogs
1	J0002-0411	00 02 41.20	-04 11 55.2	GALEXASC	—	216	—	—	—	—	1, 2, 8, 10
2	J0047+1221	00 47 11.67	+12 21 24.9	EE	—	34	140	-0.63	—	—	—
3	J0126-0118	01 26 04.13	-01 18 22.2	EE	—	389*	—	—	—	—	—
4	J0133+0957	01 33 16.94	+09 57 30.8	SDSS	0.19	27	72	-0.44	192	0.76	1, 14
5	J0141+1213	01 41 09.94	+12 13 52.0	2MASX	—	348	—	—	—	—	—
6	J0145-0820	01 45 56.65	-08 20 26.3	SDSS	0.19	42	—	—	254	—	1
7	J0204-0915	02 04 06.30	-09 15 59.8	EE	—	207	—	—	—	—	1, 2, 8, 10
8	J0204-0716	02 04 54.96	-07 16 03.3	EE	—	263	—	—	—	—	1, 2, 8, 10
9 ^a	J0206-0215	02 06 13.50	-02 15 04.1	EE	—	24	—	—	—	—	1
10	J0210-0310	02 10 30.61	-03 10 47.0	SDSS	0.24	25	—	—	240	—	1
11 ^b	J0219+0155	02 19 58.72	+01 55 48.9	2MASS	0.04 ³⁰	548	2063	-0.59	79	0.45	1, 2, 8, 9, 10
12	J0252-0756	02 52 27.53	-07 56 05.4	SDSS	0.08	112	—	—	91	—	1, 2, 13, 14
13	J0256+0016	02 56 40.12	+00 16 33.5	SDSS	—	20	92	-0.68	—	—	1
14	J0313-0631	03 13 29.05	-06 31 19.5	EE	—	80	—	—	—	—	1
15	J0325-0743	03 25 23.18	-07 43 48.5	SDSS	—	14	—	—	—	—	1
16 ^b	J0710+3546	07 10 31.01	+35 46 50.5	EE	—	76	—	—	—	—	1, 6, 12
17	J0727+4228	07 27 28.88	+42 28 00.6	SDSS	—	54	175	-0.53	—	—	1, 16
18 ^a	J0728+4935	07 28 01.48	+49 35 13.2	2MASX	0.08 ³¹	357	1531	-0.65	264	1.01	2, 10, 12
19	J0729+4142	07 29 55.79	+41 42 20.0	EE	—	117	488	-0.64	—	—	1, 2, 12, 21
20 ^a	J0738+4820	07 38 37.70	+48 20 47.9	SDSS	—	26	102	-0.61	—	—	1, 14
21	J0738+3846	07 38 54.81	+38 46 27.8	SDSS	0.32	127	—	—	776	—	2, 20
22 ^b	J0741+4618	07 41 01.91	+46 18 41.6	EE	—	230	1228	-0.75	—	—	1, 2, 10, 12, 21
23	J0746+4217	07 46 40.44	+42 17 09.2	SDSS	0.43	14	—	—	491	—	1
24	J0814+5059	08 14 31.27	+50 59 23.1	EE	—	60	329	-0.76	—	—	1, 6
25	J0816+0458	08 16 27.35	+04 58 47.6	2MASX	—	61	92	-0.18	—	—	8, 12, 22
26 ^a	J0818+2247	08 18 54.09	+22 47 44.9	SDSS	0.10	308	1113	-0.58	146	1.48	1, 2, 10, 12
27 ^a	J0831+0125	08 31 52.79	+01 25 53.3	SDSS	0.27	125	844	-0.86	468	3.88	—
28	J0832+4559	08 32 58.03	+45 59 28.2	SDSS	0.64	37	266	-0.88	710	8.38	1
29	J0839-0141	08 39 17.84	-01 41 58.1	MaxBCG	0.28	99	—	—	432	—	1
30	J0847+4934	08 47 51.14	+49 34 14.1	EE	—	234	1712	-0.89	—	—	1, 2, 10, 12
31	J0847+3147	08 47 58.65	+31 47 50.2	EE	—	164*	—	—	—	—	—
32	J0850+0153	08 50 51.71	+01 53 09.8	EE	—	50	192	-0.60	—	—	—
33	J0850+4753	08 50 53.41	+47 53 51.6	SDSS	0.18	67	273	-0.63	219	1.17	1, 2, 14
34	J0856+4951	08 56 18.72	+49 51 06.4	SDSS	0.62	37	167	-0.67	740	9.15	1
35 ^b	J0859-0252	08 59 54.15	-02 52 41.8	EE	—	402	—	—	—	—	1, 2, 4, 8, 9, 10
36 ^a	J0902+5203	09 02 36.84	+52 03 48.7	SDSS	0.10	425	2060	-0.71	229	1.75	1, 2, 6, 10, 12, 14
37	J0906+4752	09 06 20.55	+47 52 08.1	SDSS	0.24	154	—	—	446	—	14
38 ^a	J0918-0650	09 18 13.05	-06 50 59.1	EE	—	58	—	—	—	—	1
39 ^{a,b}	J0924+4034	09 24 01.17	+40 34 57.1	SDSS	0.16	320	2022	-0.82	313	3.21	1, 2, 10, 12, 14, 15, 21
40	J0926+2921	09 26 38.99	+29 21 22.6	SDSS	—	126	—	—	—	—	—
41 ^a	J0933-0310	09 33 10.69	-03 10 40.1	EE	—	75	—	—	—	—	1
42	J0940+1510	09 40 13.55	+15 10 53.2	SDSS	0.63	26	104	-0.62	685	6.98	1
43	J0941+0814	09 41 42.11	+08 14 0.5	EE	—	38	150	-0.61	—	—	—
44	J1004-0337	10 04 23.49	-03 37 26.8	EE	—	57	—	—	—	—	1
45	J1006-0621	10 06 48.08	-06 21 56.9	EE	—	267	—	—	—	—	1, 2, 8, 10
46 ^{a,b}	J1011-0607	10 11 34.79	-06 07 53.0	EE	—	36	—	—	—	—	1
47	J1011+4353	10 11 49.38	+43 53 19.1	SDSS	—	329	1611	-0.71	—	—	1, 2, 6, 10, 12, 21
48 ^a	J1014+3507	10 14 18.28	+35 07 29.1	SDSS	—	157	937	-0.80	—	—	1, 2, 7, 10, 12, 20
49 ^b	J1018+1058	10 18 04.89	+10 58 41.7	EE	—	44	186	-0.64	—	—	1
50	J1028+0345	10 28 23.47	+03 45 31.4	SDSS	0.10	287	1477	-0.73	279	1.14	1, 2, 8, 10, 12, 14
51 ^a	J1028+1943	10 28 56.38	+19 43 41.0	SDSS	0.60	231	1584	-0.86	944	46.33	15
52 ^a	J1056+1128	10 56 14.77	+11 28 42.7	SDSS	0.42	21	92	-0.66	640	2.11	1
53	J1057+3012	10 57 20.44	+30 12 30.4	SDSS	0.24	79	272	-0.55	396	2.94	23
54 ^a	J1122+2125	11 22 29.39	+21 25 02.4	EE	—	630	—	—	—	—	1, 2, 7, 9, 10, 11
55	J1127+1909	11 27 58.48	+19 09 27.3	EE	—	206	—	—	—	—	—
56 ^a	J1138+2039	11 38 50.24	+20 39 18.3	SDSS	0.18	74*	267	-0.58	225	1.35	1, 13, 14
57	J1140+1743	11 40 16.98	+17 43 40.3	SDSS	0.01	1154	3884	-0.54	12	0.07	1, 2, 4, 10, 11, 14, 15, 19
58	J1145-0227	11 45 30.97	-02 27 11.2	SDSS	0.13	148	—	—	362	—	8
59	J1149+3802	11 49 50.18	+38 02 37.0	SDSS	0.53	62	250	-0.62	533	11.35	1
60 ^{a,b}	J1156+2138	11 56 45.30	+21 38 09.1	SDSS	0.62	202	1004	-0.72	819	47.04	1, 2, 7, 12

Table 2. Candidate S/Z-Shaped Radio Sources

Catalog Number	Name	R.A. (J2000.0)	Decl. (J2000.0)	Ref.	Redshift (z)	F_{1400} (mJy)	F_{150} (mJy)	α_{150}^{1400}	Linear Size (kpc)	L (ergs $^{-1}$) ($\times 10^{42}$)	Other Catalogs
61	J1157+3012	11 57 08.30	+30 12 17.1	EE	—	34	231	-0.86	—	—	1
62 ^b	J1201+3257	12 01 51.87	+32 57 01.3	EE	—	158	—	—	—	—	6
63 ^a	J1204+5531	12 04 06.72	+55 31 14.6	SDSS	—	459	—	—	—	—	15
64 ^a	J1204+0345	12 04 25.76	+03 45 05.4	EE	—	62	220	-0.57	—	—	1
65	J1206-0621	12 06 26.31	-06 21 43.4	LCRS	—	130	—	—	—	—	1
66	J1208+2513	12 08 09.07	+25 13 57.0	EE	—	129*	257	-0.30	—	—	1
67	J1215+1709	12 15 43.82	+17 09 17.6	SDSS	0.10	488	1462	-0.49	233	2.81	1, 2, 10, 15
68	J1218+3548	12 18 19.04	+35 48 17.2	SDSS	0.25	129	576	-0.67	592	4.08	7, 10, 12, 14, 17, 20
69 ^a	J1222+3758	12 22 09.68	+37 58 55.7	EE	—	170	—	—	—	—	—
70	J1223+2542	12 23 00.24	+25 42 02.9	SDSS	0.33	23	80	-0.56	493	1.58	1, 14
71	J1232+3130	12 32 11.44	+31 30 58.1	SDSS	0.35	80	320	-0.62	533	5.82	1
72	J1234-0804	12 34 37.40	-08 04 14.0	EE	—	88	—	—	—	—	1
73 ^a	J1243-0613	12 43 34.68	-06 13 22.2	2MASX	0.14 ³²	367	—	—	357	—	1, 2, 4, 8, 9, 10, 14, 15
74 ^a	J1255+4405	12 55 54.60	+44 05 21.8	SDSS	—	51	156	-0.50	—	—	—
75	J1300-0337	13 00 31.44	-03 37 46.2	SDSS	—	170	—	—	—	—	—
76 ^a	J1303+0339	13 03 59.47	+03 39 32.3	SDSS	0.18	420	2530	-0.49	657	5.77	2, 4, 9, 10
77 ^a	J1304+2015	13 04 22.28	+20 15 56.3	SDSS	0.19	66	331	-0.72	225	1.09	1, 13, 14, 18, 23
78	J1305+3622	13 05 51.80	+36 22 53.0	MaxBCG	0.31	211	910	-0.65	417	9.85	20
79 ^a	J1307+1218	13 07 55.53	+12 18 48.3	SDSS	0.18	60	199	-0.54	275	1.13	1, 15
80 ^a	J1308-0500	13 08 39.03	-05 00 37.5	2MASX	—	272	—	—	—	—	28
81	J1310+2600	13 10 46.12	+26 00 58.5	SDSS	—	100	348	-0.56	—	—	—
82 ^a	J1319+0502	13 19 43.59	+05 02 43.0	SDSS	1.28	27	—	—	2457	—	1
83 ^a	J1320+2532	13 20 00.19	+25 32 43.8	SDSS	0.13	316	1380	-0.66	207	2.68	1, 2, 7, 14, 20
84 ^a	J1325+5736	13 25 11.19	+57 36 01.2	SDSS	0.12	110	1643	-1.21	297	0.68	14, 24, 25
85 ^a	J1327+0007	13 27 57.49	+00 07 51.3	SDSS	0.51	62	275	-0.67	949	9.61	1
86	J1328+0150	13 28 42.37	+01 50 59.5	SDSS	—	10	43	-0.65	—	—	1
87	J1337+5348	13 37 57.66	+53 48 25.2	SDSS	0.10	29	72	-0.41	121	0.23	1
88 ^a	J1339+1024	13 39 13.64	+10 24 47.9	SDSS	—	116	782	-0.85	—	—	1
89	J1345+3124	13 45 41.65	+31 24 06.4	SDSS	0.22	80	214	-0.44	258	3.05	1, 14
90 ^a	J1346+6220	13 46 17.54	+62 20 45.4	SDSS	0.12	160	673	-0.64	173	1.03	1, 2, 6, 10, 12, 15, 26, 27
91 ^a	J1349+4306	13 49 29.86	+43 06 10.2	EE	—	163	1129	-0.87	—	—	21
92	J1356+4555	13 56 59.94	+45 55 04.6	2MASX	0.24	95	355	-0.59	289	3.22	1, 21
93 ^a	J1359+6119	13 59 54.22	+61 19 45.2	SDSS	0.18	30	104	-0.56	210	0.55	1
94	J1402+4612	14 02 32.38	+46 12 33.7	SDSS	0.56	93	500	-0.75	883	16.25	1, 2, 12, 15, 21
95	J1404+3701	14 04 11.63	+37 01 26.6	EE	—	26	142	-0.76	—	—	1
96 ^a	J1410+3014	14 10 50.88	+30 14 09.6	2MASX	0.18 ³³	84	235	-0.46	338	1.84	1, 18
97	J1411+4535	14 11 10.93	+45 35 18.1	EE	—	35	86	-0.40	—	—	1
98	J1417+0812	14 17 31.27	+08 12 30.1	SDSS	0.06	352	—	—	208	—	2, 14, 15, 19
99 ^a	J1418+0952	14 18 13.47	+09 52 38.5	SDSS	0.34	333	692	-0.33	622	42.84	1, 2, 16
100 ^a	J1418+3530	14 18 40.50	+35 30 01.6	2MASX	—	90	194	-0.34	—	—	1
101 ^a	J1426+2158	14 26 23.01	+21 58 39.5	SDSS	0.20	81	—	—	359	—	1
102	J1426+3411	14 26 59.61	+34 11 59.6	SDSS	0.13	304	—	—	326	—	15
103	J1437+1616	14 37 16.71	+16 16 04.1	SDSS	0.27	38	—	—	493	—	1
104	J1439+1106	14 39 28.37	+11 06 02.7	EE	—	43	115	-0.44	—	—	1
105	J1442+5043	14 42 19.18	+50 43 57.9	SDSS	0.17	205	878	-0.65	326	3.04	1, 17
106	J1524+1627	15 24 19.50	+16 27 12.4	SDSS	0.15	191	262	-0.14	247	7.35	14
107	J1526+0053	15 26 42.05	+00 53 28.8	SDSS	0.12	236	612	-0.43	165	2.35	1, 2, 8, 12
108	J1529-0629	15 29 19.98	-06 29 21.5	EE	—	109	—	—	—	—	1
109	J1530+3301	15 30 22.23	+33 01 19.5	EE	—	12	41	-0.55	—	—	1
110	J1530-0703	15 30 58.88	-07 03 32.4	2MASS	—	147	—	—	—	—	—
111	J1536+2357	15 36 38.05	+23 57 06.1	SDSS	0.51	59	410	-0.87	767	7.89	1
112	J1536-0453	15 36 55.69	-04 53 50.0	EE	—	25	—	—	—	—	1
113 ^a	J1540+1110	15 40 13.80	+11 10 08.6	EE	—	27	118	-0.66	—	—	1
114 ^a	J1553-0323	15 53 06.36	-03 23 18.5	EE	—	134	—	—	—	—	—
115	J1604+2355	16 04 56.66	+23 55 57.6	SDSS	0.03	661	—	—	122	—	1, 2, 4, 14, 15, 19
116 ^a	J1608+4309	16 08 04.52	+43 09 48.5	SDSS	0.08	76	224	-0.48	96	0.35	1, 13, 14
117	J1608+3505	16 08 29.68	+35 05 53.8	SDSS	0.35	37	153	-0.64	506	2.60	1
118	J1613+1921	16 13 35.02	+19 21 05.8	SDSS	—	195	803	-0.63	—	—	—
119	J1617+1420	16 17 52.73	+14 20 17.2	SDSS	—	37	156	-0.64	—	—	1

Table 2. Candidate *S/Z*-Shaped Radio Sources

Catalog Number	Name	R.A. (J2000.0)	Decl. (J2000.0)	Ref.	Redshift (z)	F_{1400} (mJy)	F_{150} (mJy)	α_{150}^{1400}	Linear Size (kpc)	L (ergs^{-1}) ($\times 10^{42}$)	Other Catalogs
120	J1633+4220	16 33 13.40	+42 20 31.3	SDSS	0.12	110	179	-0.22	197	2.00	1, 12, 14, 21
121 ^a	J1643+2642	16 43 18.86	+26 42 35.3	EE	—	68	330	-0.71	—	—	1
122	J1649+5358	16 49 34.80	+53 58 16.0	2MASX	—	176	542	-0.50	—	—	—
123 ^a	J1728+4200	17 28 43.50	+42 00 06.5	EE	—	31	—	—	—	—	—
124	J2107-0203	21 07 44.25	-02 03 40.4	EE	—	48	—	—	—	—	1
125	J2129-0549	21 29 00.88	-05 49 52.9	EE	—	33	—	—	—	—	1
126	J2137-0811	21 37 25.01	-08 11 05.6	SDSS	—	57	—	—	—	—	1
127	J2159-0211	21 59 15.62	-02 11 25.3	SDSS	0.30	58	—	—	332	—	1
128	J2210+1050	22 10 21.47	+10 50 55.4	EE	—	63	265	-0.64	—	—	1, 2
129	J2250-0439	22 50 56.53	-04 39 41.1	EE	—	30	—	—	—	—	1
130	J2306-0341	23 06 27.76	-03 41 23.3	EE	—	51	—	—	—	—	1
131	J2307+1253	23 07 16.28	+12 53 31.3	SDSS	0.22	57	206	-0.57	234	1.67	1, 12
132	J2321-0912	23 21 21.90	-09 12 42.8	SDSS	—	46	—	—	—	—	1
133 ^a	J2322-0941	23 22 08.20	-09 41 53.1	EE	—	125	—	—	—	—	1
134	J2331-0129	23 31 13.39	-01 29 13.2	EE	—	328	—	—	—	—	16
135 ^a	J2339+0042	23 39 00.34	+00 42 57.8	SDSS	0.18	29	—	—	260	—	1, 13, 14, 16

References— 1: NVSS (Condon et al. 1998); 2: VLSS (Cohen et al. 2007); 3: 3C (Bennett 1962; Edge et al. 1959); 4: 4C (Pilkington & Scott 1965; Gower et al. 1967; Caswell & Crowther 1969); 5: 5C (Kenderdine et al. 1966; Pooley & Kenderdine 1968; Pooley 1969; Willson 1970; Pearson 1975; Waggett 1977; Pearson & Kus 1978; Schuch 1981; Benn et al. 1982, 1988); 6: 6C (Baldwin et al. 1985; Hales et al. 1988, 1990, 1991, 1993a,b); 7: 7C (McGilchrist et al. 1990; Kollgaard et al. 1994; Waldram et al. 1996; Vessey & Green 1998); 8: PMN (Griffith et al. 1994); 9: PKS (Bolton et al. 1964); 10: TXS (Douglas et al. 1996); 11: Cul (Slee 1995); 12: 87GB (Gregory & Condon 1991); 13: ASK (Sánchez et al. 2011); 14: 2MASX (Skrutskie et al. 2006); 15: GALEXASC (Agüeros et al. 2005); 16: GALEXMSC (Agüeros et al. 2005); 17: GMBGC (Hao et al. 2010); 18: MaxBCG (Koester et al. 2007); 19: NGC (Dreyer 1888); 20: B2 (Colla et al. 1970, 1972, 1973; Fanti et al. 1974); 21: B3 (Ficarra et al. 1985); 22: RC (Goss et al. 1992); 23: WHL (Wen et al. 2010); 24: MGC (Vorontsov-Vel'Yaminov & Arkhipova 1962); 25: ABELL (Abell 1958; Abell et al. 1989); 26: WISE (Chung et al. 2011; Rebull et al. 2011); 27: WB (White & Becker 1992); 28: APMUKS (Maddox et al. 1990); 29: GIN (Wegner et al. 1996); 30: Falco et al. (1999); 31: Machalski (1998); 32: Jones et al. (2009); 33: Rykoff et al. (2012); SSTSL2 (Capak et al. 2013); LCRS (Shectman et al. 1996); TONS08 (Brand et al. 2003); TONS08w (Brand et al. 2005)

Notes— ^a The source is present in Proctor (2011).

^b The source is cataloged as an XRG by Yang et al. (2019).

* The FIRST flux (at 1400 MHz) is used instead of the NVSS flux (at 1400 MHz).